Web-based Supplementary Materials for "Evolutionary State-Space Model and Its Application to Time-Frequency Analysis of Local Field Potentials"

May 1, 2017

1 Web Appendix A

Proof of AR(2) spectral decomposition theorem

~~The lemma below gives us an explicit form of the autocovariance function of an AR(2) process. Such results will be applied in establishing the main theorem~~.

Lemma 1. *Given a (weakly) stationary zero mean AR(2) process S_t, the autocovariance function $\gamma_S(h)$ takes the form*

$$\gamma_S(h) = A_1(\rho e^{\psi i})^{-h} + A_2(\rho e^{-\psi i})^{-h}, \tag{1}$$

where A_1, A_2 can be determined by solving the linear equation $A_1 + A_2 = \frac{(1-\phi_2)\sigma_w^2}{(1+\phi_2)(1-\phi_1-\phi_2)(1+\phi_1-\phi_2)}$ and $A_1(\rho e^{\psi i})^{-1} + A_2(\rho e^{-\psi i})^{-1} = \frac{\phi_1\sigma_w^2}{(1+\phi_2)(1-\phi_1-\phi_2)(1+\phi_1-\phi_2)}$.

The proof is due to the fact that $\gamma_S(h) = \phi_1\gamma_S(h-1) + \phi_2\gamma_S(h-2)$.

~~To prove the theorem, we first claim~~ that for any fixed M, $\{f_{S^{(j)}}(\omega)\}_{j=1}^{M}$ are linearly independent.

In fact, suppose there ~~exists~~ some constants $b_1, \cdots, b_M$ such that $\sum_{j=1}^{M} b_j f_{S^{(j)}}(\omega) = 0$, then we must have $\sum_{j=1}^{M} b_j \sum_{h=-\infty}^{\infty} \gamma_{S^{(j)}}(h) e^{2\pi i\omega h} = \sum_{h=-\infty}^{\infty} \sum_{j=1}^{M} b_j \gamma_{S^{(j)}}(h) e^{2\pi i\omega h} = 0$. As a direct result from Fourier theorem, we have $\sum_{j=1}^{M} b_j \gamma_{S^{(j)}}(h) = 0$ for any h. Thus for any positive integer H, $b_1, \cdots, b_M$ are solutions of the linear equation

$$\Gamma \mathbf{b} = 0, \tag{2}$$

where $\Gamma = \begin{bmatrix} \gamma_{S^{(1)}}(0) & \gamma_{S^{(2)}}(0) & \dots & \gamma_{S^{(M)}}(0) \\ \gamma_{S^{(1)}}(1) & \gamma_{S^{(2)}}(1) & \dots & \gamma_{S^{(M)}}(1) \\ \vdots & \vdots & \vdots & \vdots \\ \gamma_{S^{(1)}}(H) & \gamma_{S^{(2)}}(H) & \dots & \gamma_{S^{(M)}}(H) \end{bmatrix}_{(H+1)*M}$ and $\mathbf{b} = (b_1, \cdots, b_M)'$. From Lemma 1, it is easy to show that $\gamma_{S^{(j)}}(h) = (\rho^{(j)})^{-h}(A_1^{(j)} + A_2^{(j)})cos(h\psi^{(j)})$. Note that due to the ~~condition~~ $\max_M\{|\omega_1 - \omega_0|, \cdots, |\omega_M - \omega_{M-1}|\} \to 0$ and $A_1^{(j)}, A_2^{(j)}$ are nonlinear functions of j, we have $\cancel{rank}(\Gamma) = \cancel{min}\{H+1, M\}$. It implies $\mathbf{b} = \mathbf{0}$ and $\{f_{S^{(j)}}(\omega)\}_{j=1}^{M}$ are linearly independent. Then we can implement the Gram-Schmidt process on the family of functions $\{f_{S^{(j)}}(\omega)\}_{j=1}^{\infty}$ to obtain a family of orthonormal functions $\{\tilde{f}_{S^{(j)}}(\omega)\}_{j=1}^{\infty}$ in $L^2(0, \frac{1}{2})$. It follows that for any nonnegative coefficients $a_1, \cdots, a_M$, there exist $\tilde{a}_1, \cdots, \tilde{a}_M$ such that $||f_Y(\omega) - \sum_{j=1}^{M} a_j^2 f_{S^{(j)}}(\omega)||_2 = ||f_Y(\omega) - \sum_{i=1}^{M} \tilde{a}_j^2 \tilde{f}_{S^{(j)}}(\omega)||_2$. If we can show $\{\tilde{f}_{S^{(j)}}(\omega)\}_{j=1}^{\infty}$ is also complete in $L^2(0, \frac{1}{2})$, by Parseval equality, we can obtain that $||f_Y(\omega) - \sum_{j=1}^{M} \tilde{a}_j^2 \tilde{f}_{S^{(j)}}(\omega)||_2 \to 0$ as $M \to \infty$ and equivalently, $||f_Y(\omega) - f_{\hat{Q}_{t,M}}(\omega)||_2 \to 0$ as $M \to \infty$.

To show that $\{\tilde{f}_{S^{(j)}}(\omega)\}_{j=1}^{\infty}$ is complete in $L^2(0, \frac{1}{2})$, it suffices to show $\{f_{S^{(j)}}(\omega)\}_{j=1}^{\infty}$ is complete. ~~Let us define~~ $\mathbb{B} = \{f_{S^{(j)}}(\omega)\}_{j=1}^{\infty}$. For any function $g(\omega)$ in $L^2(0, \frac{1}{2})$, if $g(\omega) \perp \mathbb{B}$, then we have $\int_0^{\frac{1}{2}} g(\omega) f_{S^{(j)}}(\omega) d\omega = 0$ for any j. ~~It~~ is equivalent to $\sum_{h=\infty}^{\infty} \int_0^{\frac{1}{2}} g(\omega)\gamma_{S^{(j)}}(h) e^{2\pi i \omega h} d\omega = \sum_{h=-\infty}^{\infty} \gamma_g(h)\gamma_{S^{(j)}}(h) = 0$ for any j. It boils down to the problem of solving for the linear equation

$$\Gamma' \gamma = 0, \tag{3}$$

where Γ is defined in Equation (2) and $\gamma = (\gamma_g(0), \cdots, \gamma_g(H))$ for any M and H. We have proved that Γ is of full row rank and thus $\gamma_g(h) = 0$ for any h. Thus $\{f_{S^{(j)}}(\omega)\}_{j=1}^{\infty}$ is complete in $L^2(0, \frac{1}{2})$. $\square$

2 Web Figure 1

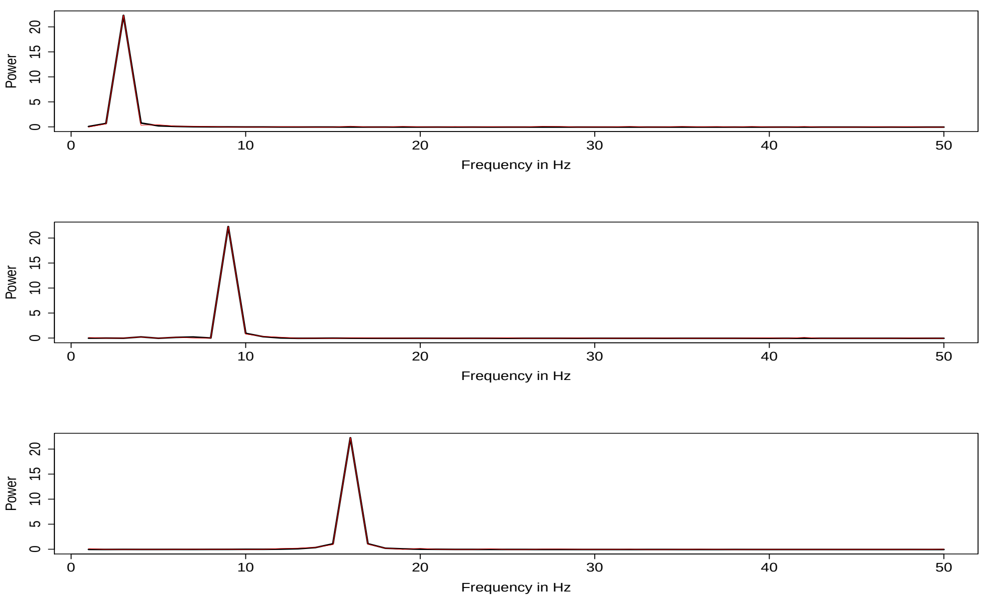

Figure 1: The periodograms of the true (black) and estimated (red) latent processes.

3 Web Figure 2

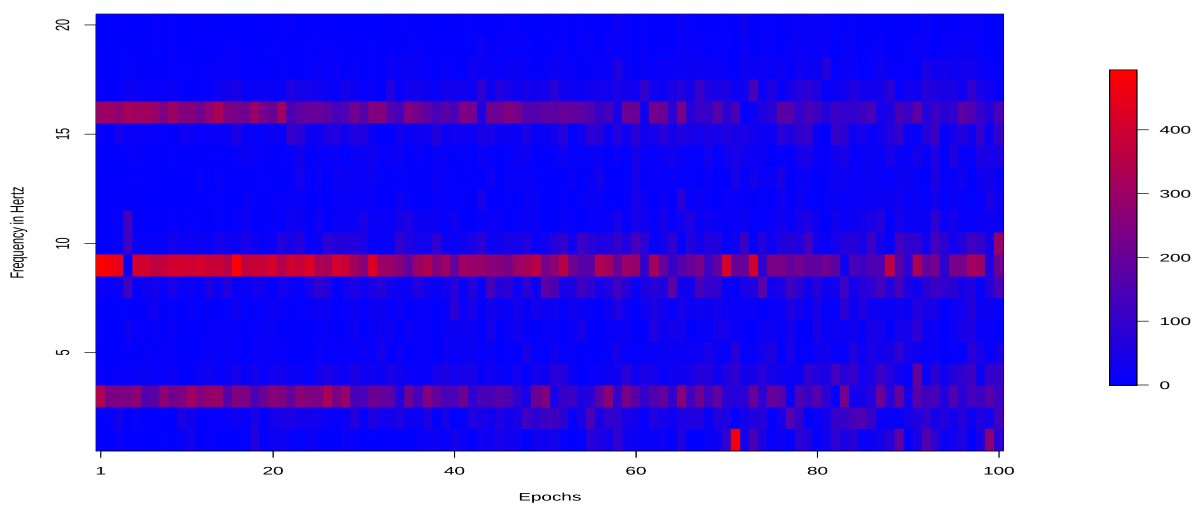

Figure 2: The periodogram of generated signals from electrode 1 computed over all 100 epochs. From the heat map, we are observing the powers are evolving across epochs. At early stage, three dominating frequency bands can be identified clearly. As epoch evolves, such pattern is getting less clear.

4 Web Figure 3

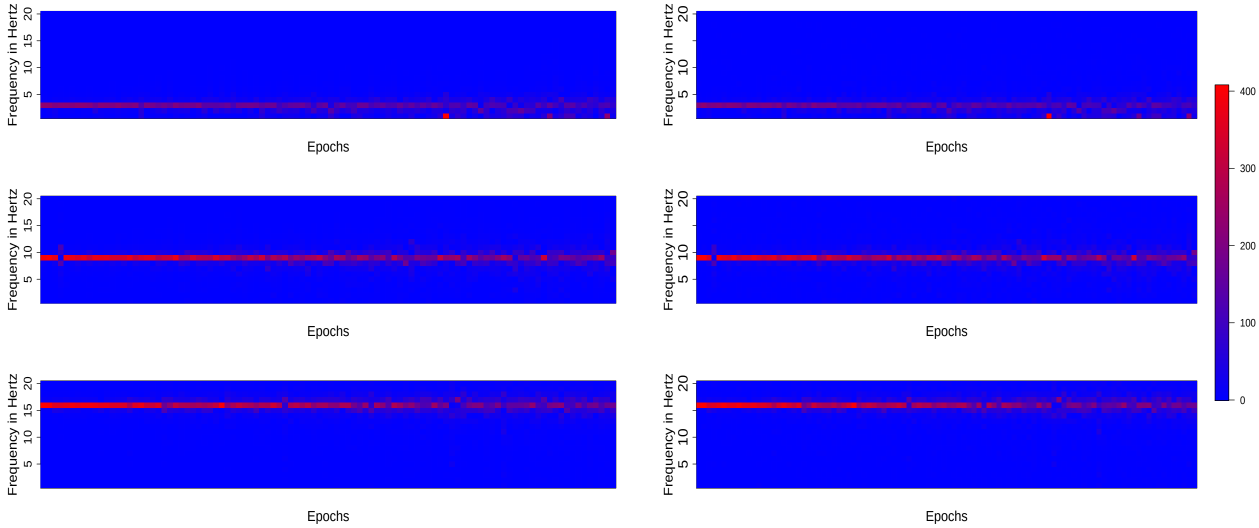

Figure 3: The periodograms of the true (left) and estimated (right) latent AR(2) processes corresponding to delta (top), alpha (middle) and beta (bottom) frequency band.

5 Web Figure 4

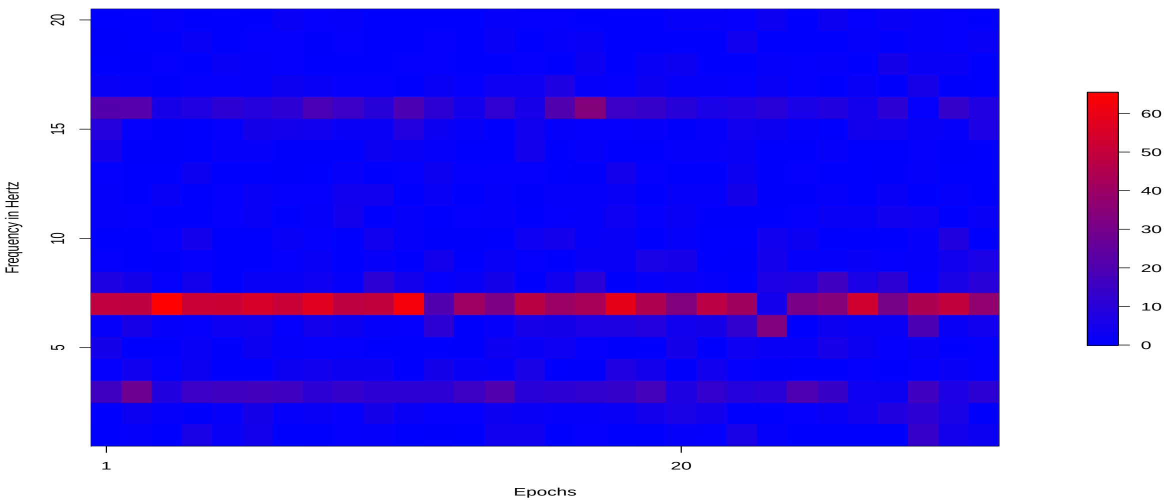

Figure 4: The periodogram of generated signals from electrode 1 computed over all 30 epochs.

6 Web Figure 5

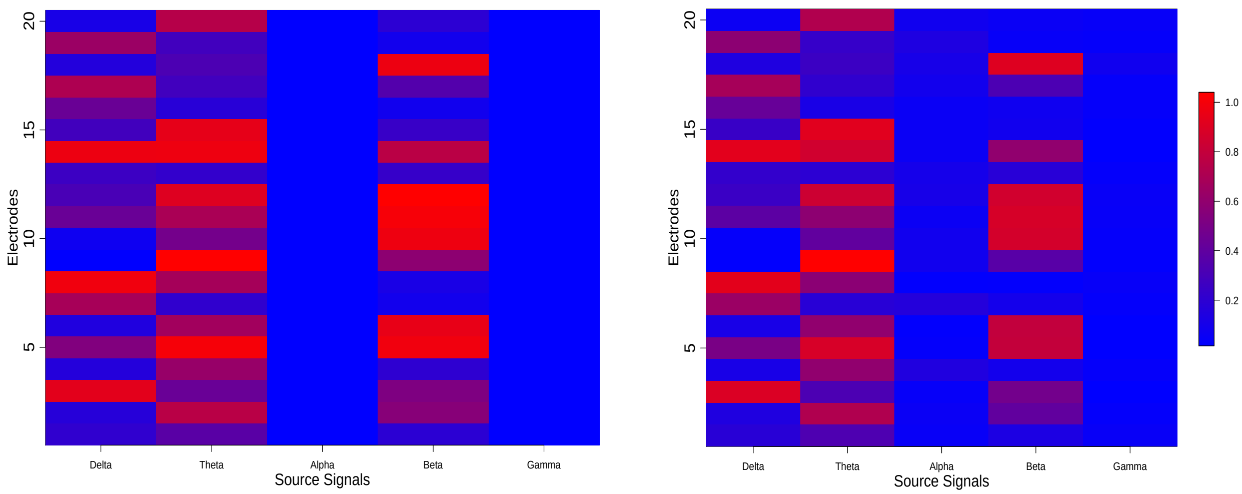

Figure 5: The true mixing matrix (left) and estimated mixing matrix (right). Darker color indicates heavier weight given by the corresponding latent processes. Columns corresponding to "alpha" and "gamma" bands are zero in the true mixing matrix (left). In the estimated mixing matrix (right), those two columns are also close to zero.

7 Web Figure 6

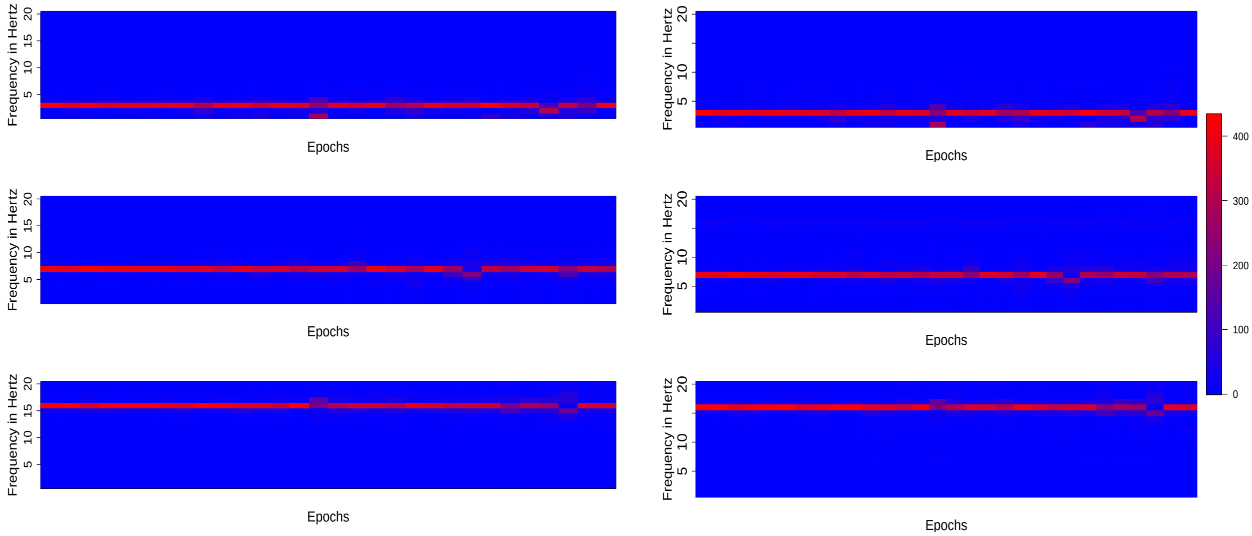

Figure 6: The periodograms of the true (left) and estimated (right) latent AR(2) processes corresponding to delta (top), theta (middle) and beta (bottom) frequency band.

8 Web Figure 7

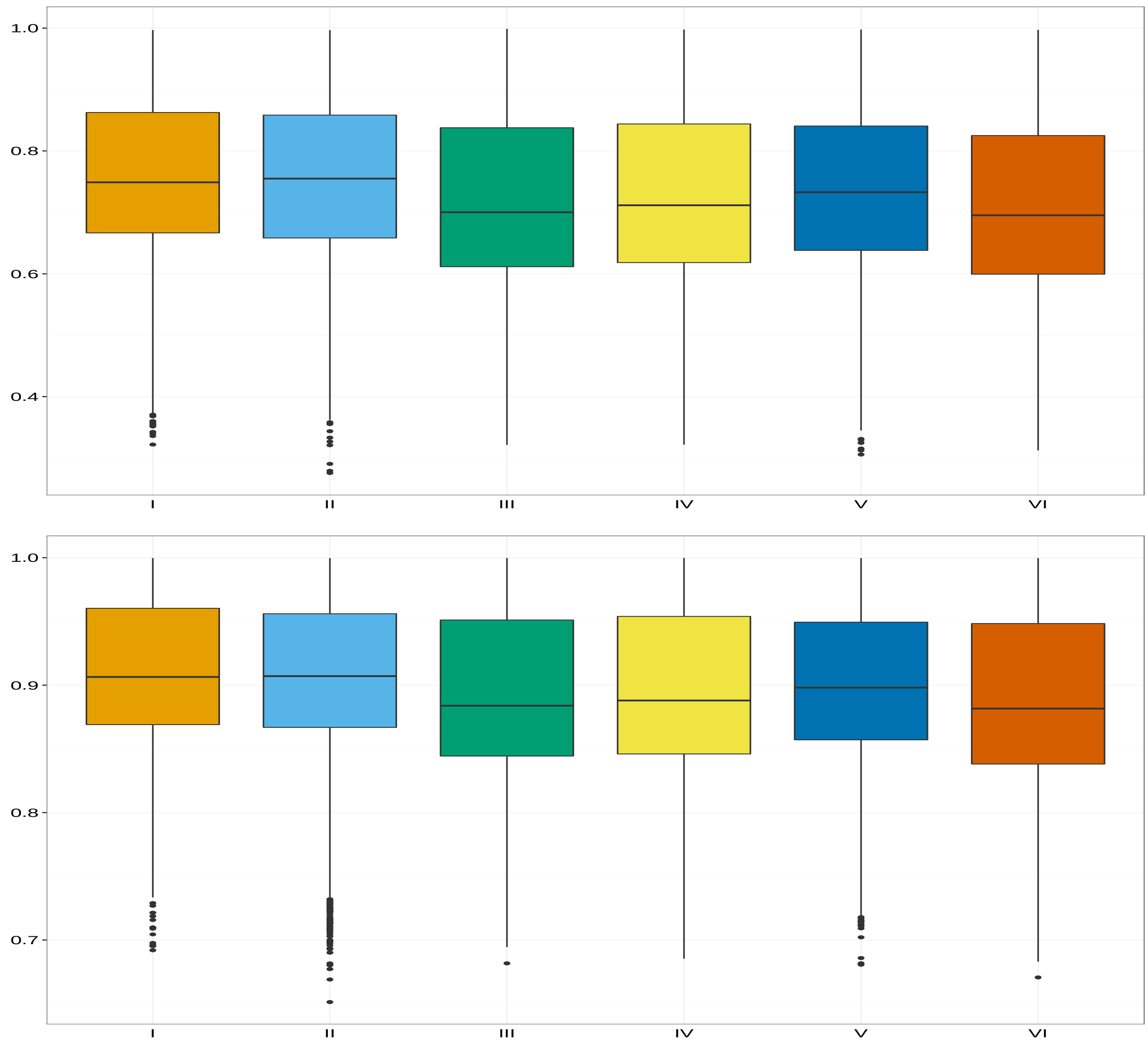

Figure 7: The boxplots of variance accounted by different components across different stages during the experiment. The results were obtained by conducting principal component analysis on frequency domain. Epochs in the entire experiment have been classified as 6 stages with each consisting of 40 epochs (Stage I: 1-40, II: 41-80, III: 81-120, IV: 121-160, V: 161-200, VI: 201-247). The first component is shown on top and the first three cumulative components is at the bottom. We could observe that about 90% of variance can be explained by three components.

9 Web Figure 8

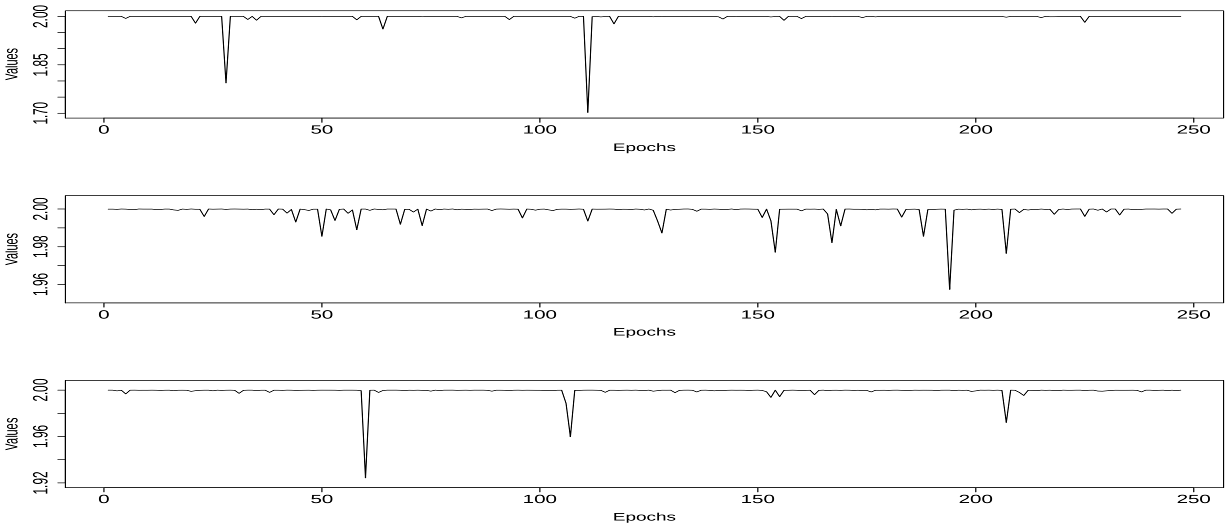

Figure 8: The time series plots of modulus corresponding to delta (above), alpha (middle) and gamma (bottom) frequency bands.

10 Web Figure 9

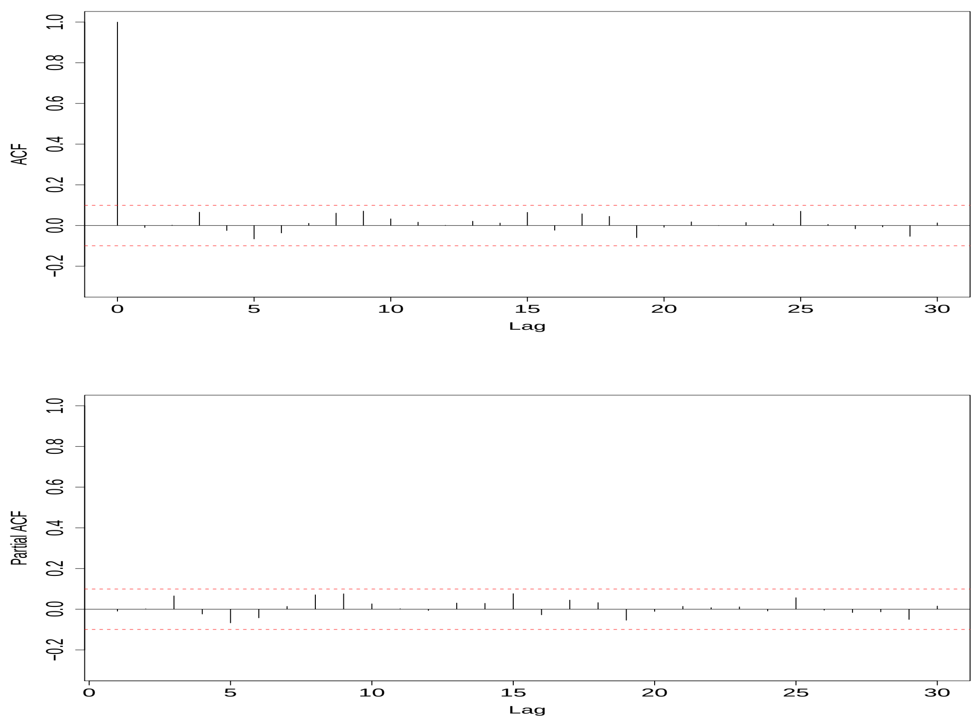

Figure 9: Top: Auto-correlation function (ACF) of the residual plots from electrode 1. Bottom: Partial auto-correlation function (PACF) of the residual plots from electrode 1. The dashed lines indicate the threshold for non-zero correlation. These plots, along with the Ljung-Box test for white noise ($p - value \approx 0.75$) suggest that the residuals are white noise and hence the E-SSM model fits the data well. These same plots were observed in all the other electrodes but we do not report them here due to space constraints.